

Supporting information

Water-Resistant 2D Lead(II) Iodide Perovskites: Correlation
Between Optical Properties and Phase Transitions

Bhushan P. Kore and James M. Gardner

Department of Chemistry, Division of Applied Physical Chemistry, KTH Royal Institute of
Technology,

SE-100 44 Stockholm, Sweden

Corresponding author's e-mail address: jgardner@kth.se

Materials

$C_{14}H_{29}NH_2$ (95%), $C_{16}H_{33}NH_2$ (98%), $C_{18}H_{37}NH_2$ (99%), PbI_2 (99.99%), Hydroiodic (HI) acid (57% in water), N, N-Dimethylformamide (DMF, anhydrous, 99.8%) and Dimethyl sulfoxide (DMSO, anhydrous, $\geq 99.9\%$) were purchased from Sigma Aldrich. Ethanol (98%) was purchased from Fisher Scientific. All chemicals were used as received without any further purification.

Synthesis of $(C_{14}H_{29}NH_3)_2PbI_4$, $(C_{16}H_{33}NH_3)_2PbI_4$ and $(C_{18}H_{37}NH_3)_2PbI_4$

0.992 g (2 mmol) of PbI_2 was dissolved in 2 ml (57% in water) Hydroiodic (HI) acid in a glass vial. In second step the mixture of 0.854 g (4 mmol) of $C_{14}H_{29}NH_2$ in 5 ml HI and 50 ml ethanol was stirred continuously for nearly 30 mins, then the solution of the reaction mixture was increased to 60 °C. The PbI_2 solution in HI was then dropwise added to the solution in step 2 under continuous stirring. The final mixture was refluxed for 45 mins followed by a slow cooling (5 °C/hour) to room temperature.^[1,2] Needle shape single crystals were obtained. The single crystal were filtered, washed with diethyl ether and finally dried in vacuum.

A nearly similar procedure was adopted for the synthesis of $(C_{16}H_{33}NH_3)_2PbI_4$ and $(C_{18}H_{37}NH_3)_2PbI_4$ where in first step 2 mmol of PbI_2 was dissolved in 2 ml HI and in second step 4 mmol of $C_{16}H_{33}NH_4$ and $C_{18}H_{37}NH_4$ was dissolved in 5 ml HI and 75 ml ethanol, respectively. The other synthesis conditions were same as mentioned for the synthesis of $(C_{14}H_{29}NH_3)_2PbI_4$.

Thin film fabrication

The 2D perovskite crystals were dissolved in 0.5 ml DMF:DMSO (4:1) mixture solution and stirred at room temperature for 10-15 min. A 70 μ l solution of perovskite was then spin coated on pure glass or F-doped SnO_2 glass/mesoporous TiO_2 (Meso TiO_2) substrates at 3000 rpm for 30 sec. The films were then annealed at 100 °C for 15-20 min. For spin coating onto the Meso TiO_2 layer, a TiO_2 colloidal precursor solution^[3] was diluted with absolute ethanol and spin coated on FTO substrate at 3000 rpm for 30 sec followed by heating at 80 °C for 20 min. The final annealing was carried out in a muffle furnace where the films were annealed at 450 °C for 1 hour.^[3]

Characterization

Differential scanning calorimetry (DSC) measurements were carried out on Mettler Toledo DSC823 system in the temperature range of 280 to 400 K in N_2 atmosphere with heating and cooling rates 3°C/min. X-ray diffraction (XRD) patterns were measured on X'Pert PRO, PANalytical using CuK_{α} radiation ($\lambda = 1.5406 \text{ \AA}$) to analyse the purity of the prepared sample and to determine the phase and crystal structure of the prepared materials. The ultraviolet-visible (UV-Vis) absorption spectra were recorded on a Varian Cary 300 Bio UV-Vis spectrophotometer. The steady-state photoluminescence spectra were recorded on a Varian Cary Eclipse fluorescence spectrophotometer. The absolute quantum yield of the samples were measured using an integrating sphere coupled with a fluorescence spectrometer.

Absolute and relative photoluminescence quantum yield measurements:

The absolute quantum yield of 2D perovskite powder samples was measured using an integrating sphere coupled with the spectrometer. For measurements the perovskite samples were placed at the center of sphere on the sample stage. The samples were then excited at 365 nm. The visible light emitted by perovskite samples was then detected by spectrometer that was coupled to integrating sphere. To quantify the quantum yields the scattering from the blank sample holder was also measured. Finally, the PL QYs were estimated by comparing integrated PL emission intensity with scattering from the reference.

For relative PL QY measurements a standard sample with known quantum yield was used as a reference, for our measurements we used Coumarin 6 as a reference. The relative quantum yield (Φ_s) of a sample is given by,^[4]

$$\Phi_s = \Phi_r \frac{I_s A_r n_s^2}{I_r A_s n_r^2} \dots\dots\dots(1)$$

where 'I' is integrated emission intensity, 'A' is absorption intensity at excitation wavelengths and 'n' is refractive index. The subscript s and r refer to the sample and reference dye with a known quantum efficiency Φ_r .

For reference, a dilute solution of Coumarin 6 in ethanol was prepared and used for relative quantum yield measurements. The 2D perovskite samples spin coated on glass substrate were used for relative quantum yield measurements.

The relative quantum yields of the perovskite samples with respect to the known quantum yield of Coumarin 6 in ethanol (0.78) are then calculated using equation (1).

The relative quantum yield values are higher compared to the PL QYs estimated from the absolute quantum yield measurements. The PL QY measurements on the powdered samples is limited by the inhomogenous light absorption by the solid samples. As well, the PL QYs in solid samples depend upon the grain size and crystallinity of the sample. From the XRD patterns, it is clear that the crystal phases are anisotropic for the thin film samples, which is not the case for the powder samples. We believe that the PL QYs that we have measured represent the lower limit for these materials, due to the light scattering and anisotropy of the thin films and reabsorption losses in powder samples.

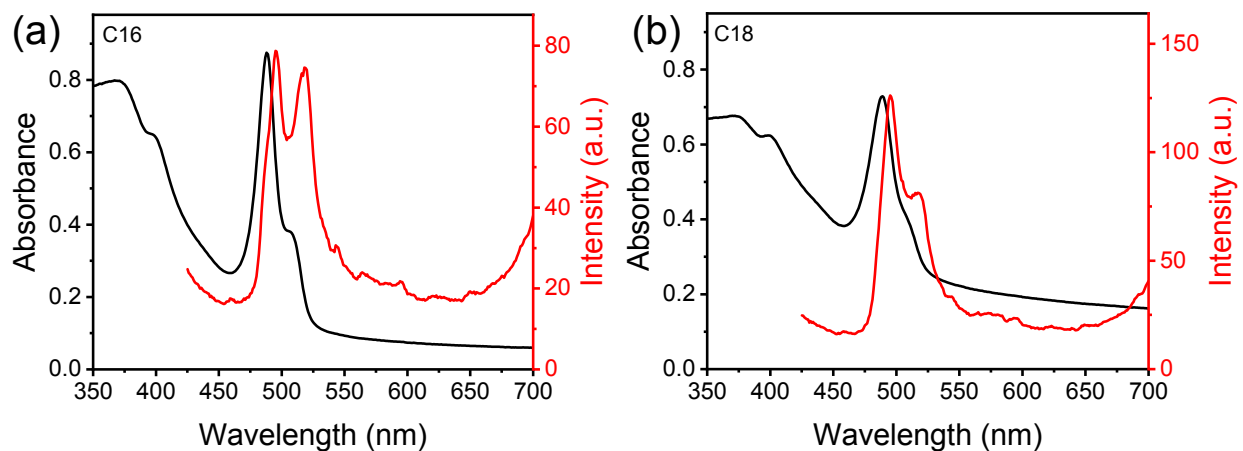


Figure S1. Absorption and photoluminescence spectra of (a) $(\text{C}_{16}\text{H}_{33}\text{NH}_3)_2\text{PbI}_4$ and (b) $(\text{C}_{18}\text{H}_{37}\text{NH}_3)_2\text{PbI}_4$ 2D perovskite thin films annealed at 100 °C.

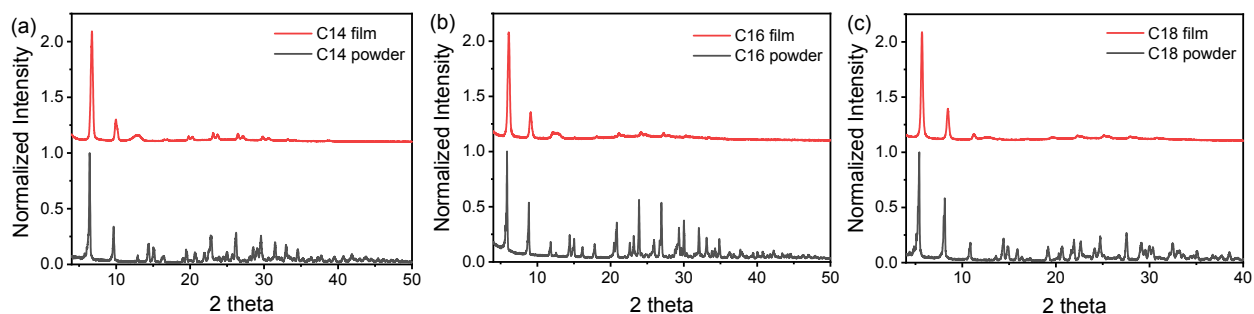


Figure S2. Comparison of XRD pattern of $(\text{C}_{14}\text{H}_{29}\text{NH}_3)_2\text{PbI}_4$, $(\text{C}_{16}\text{H}_{33}\text{NH}_3)_2\text{PbI}_4$ and $(\text{C}_{18}\text{H}_{37}\text{NH}_3)_2\text{PbI}_4$ 2D perovskites measured on thin films and powder sample.

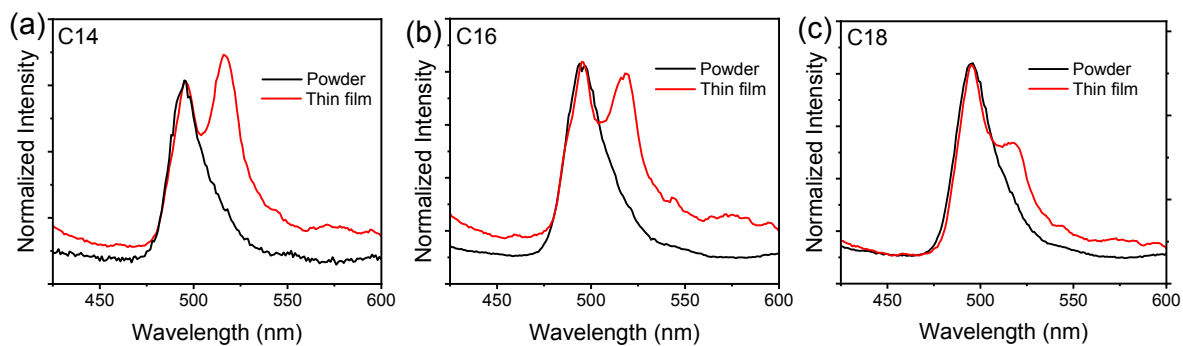


Figure S3. Comparison of photoluminescence spectra of $(\text{C}_{14}\text{H}_{29}\text{NH}_3)_2\text{PbI}_4$, $(\text{C}_{16}\text{H}_{33}\text{NH}_3)_2\text{PbI}_4$ and $(\text{C}_{18}\text{H}_{37}\text{NH}_3)_2\text{PbI}_4$ 2D perovskites as powders and thin films.

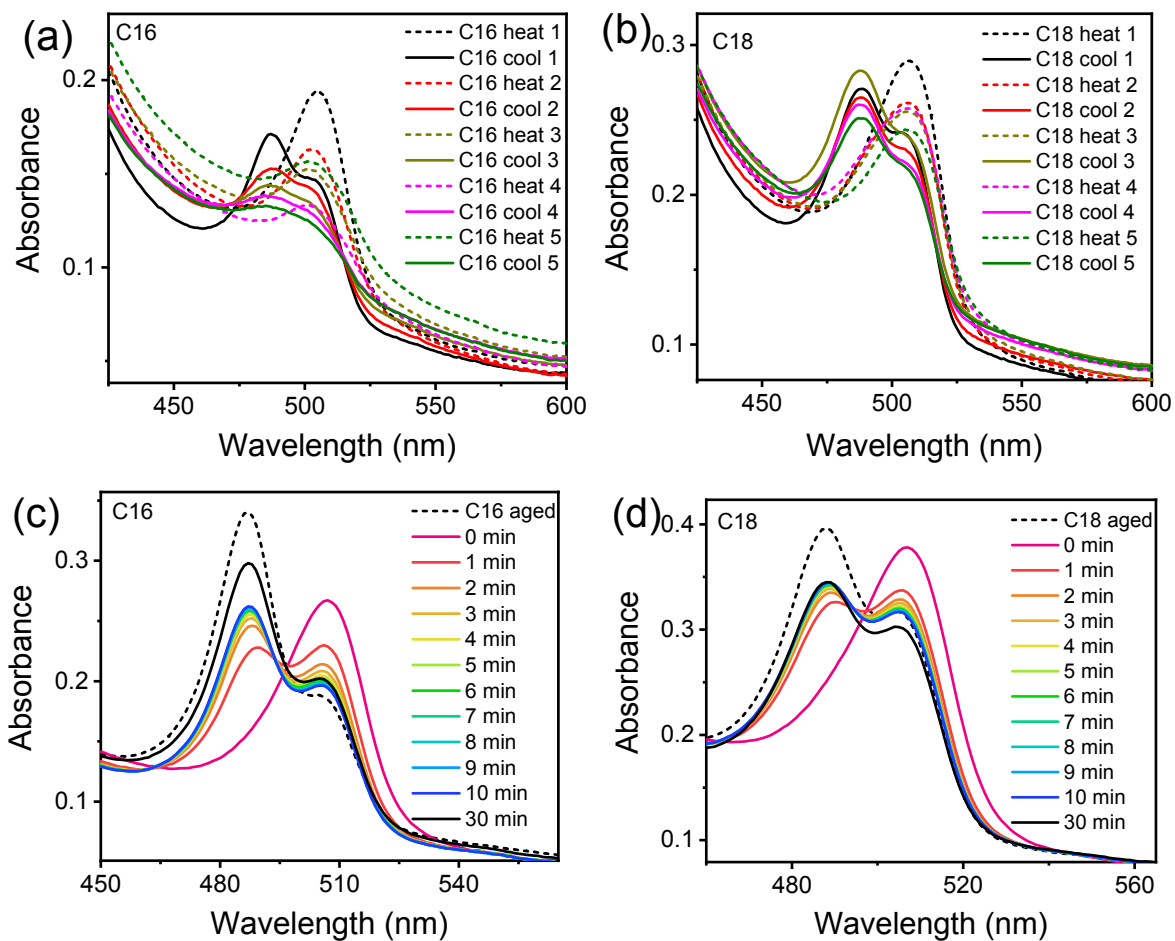


Figure S4. Absorption spectra of (a) $(C_{16}H_{33}NH_3)_2PbI_4$ and (b) $(C_{18}H_{37}NH_3)_2PbI_4$ 2D perovskite thin films recorded just after annealing the thin film at 100 °C (dotted curve) and thin film cooled to room temperature for 1hr (solid curve). Evolution of absorption spectra of (c) $(C_{16}H_{33}NH_3)_2PbI_4$ and (d) $(C_{18}H_{37}NH_3)_2PbI_4$ 2D perovskite thin films just after annealing at 100 °C with time.

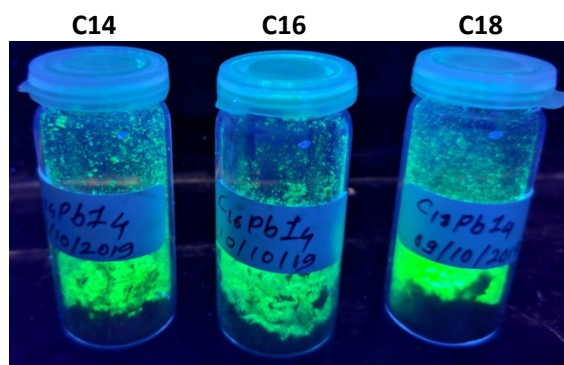


Figure S5. Bright green light photoluminescence from the $(C_{14}H_{29}NH_3)_2PbI_4$, $(C_{16}H_{33}NH_3)_2PbI_4$ and $(C_{18}H_{37}NH_3)_2PbI_4$ 2D perovskites powder samples under continuous 365 nm illumination.

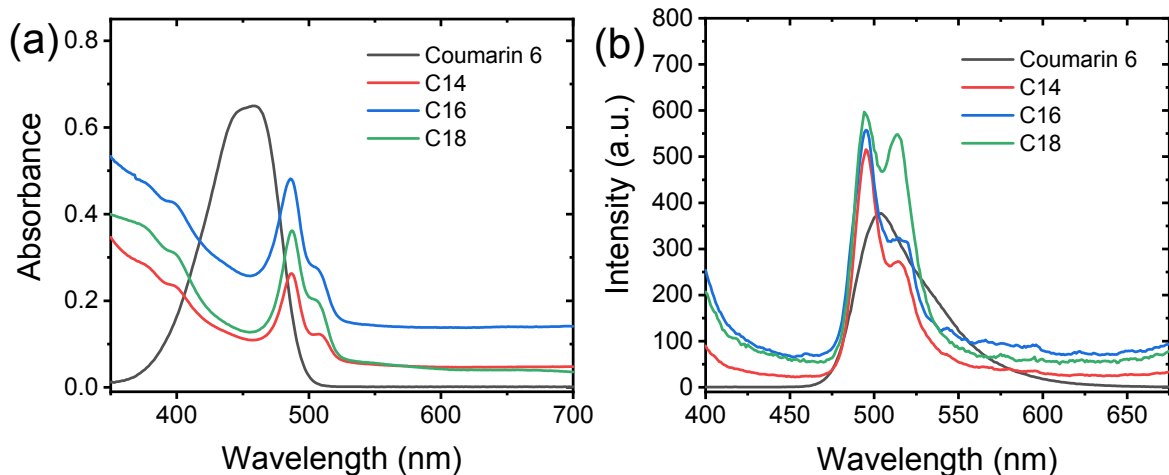


Figure S6. (a) Optical absorption and (b) photoluminescence spectra of $(C_{14}H_{29}NH_3)_2PbI_4$, $(C_{16}H_{33}NH_3)_2PbI_4$ and $(C_{18}H_{37}NH_3)_2PbI_4$ 2D perovskite thin films along with a reference dye Coumarin 6. The relative photoluminescence quantum yield of 2D perovskite samples are calculated with respect to known quantum yield of Coumarin 6 (78%).

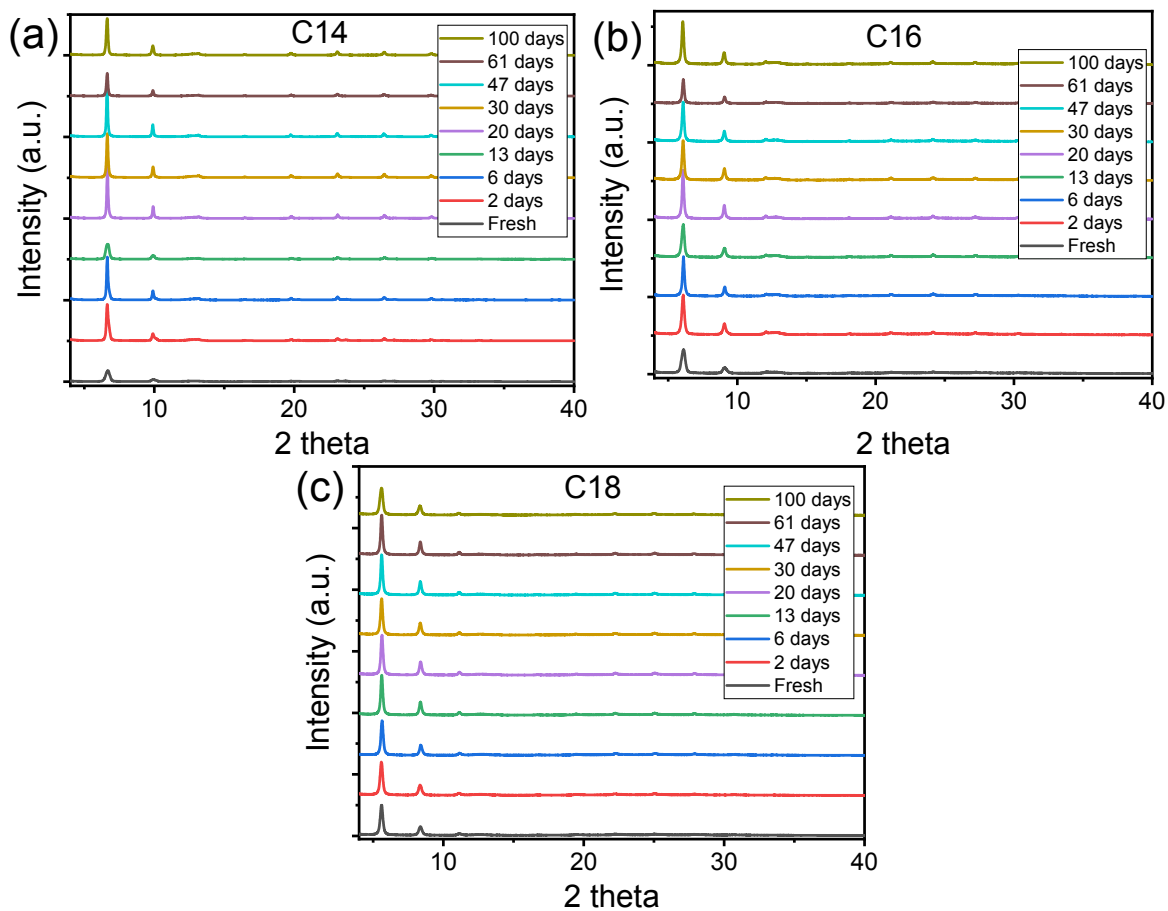


Figure S7. XRD pattern of thin films of $(C_{14}H_{29}NH_3)_2PbI_4$, $(C_{16}H_{33}NH_3)_2PbI_4$ and $(C_{18}H_{37}NH_3)_2PbI_4$ 2D perovskite thin films stored under ambient conditions.

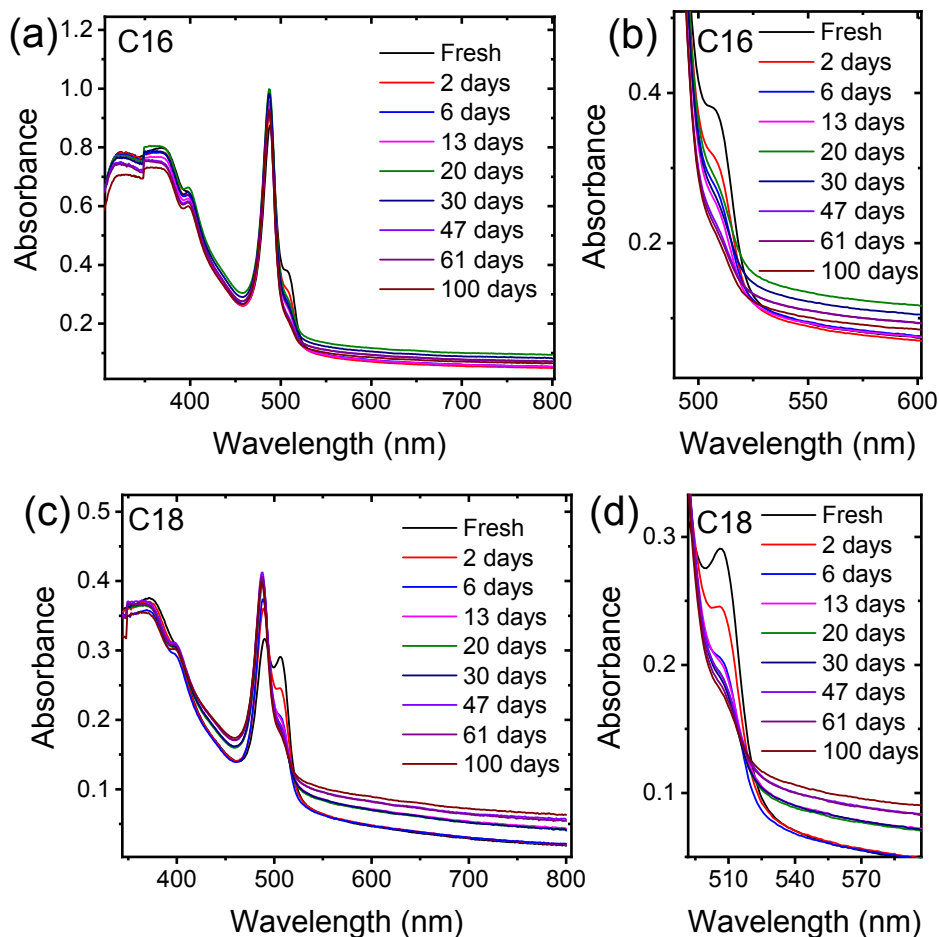


Figure S8. Absorption spectra of thin films of (a) $(C_{16}H_{33}NH_3)_2PbI_4$, (b) magnified view of the absorption peak at longer wavelength of $(C_{16}H_{33}NH_3)_2PbI_4$ and (c) $(C_{18}H_{37}NH_3)_2PbI_4$ (d) magnified view of the absorption peak at longer wavelength of $(C_{18}H_{37}NH_3)_2PbI_4$ 2D perovskite thin films stored under ambient conditions.

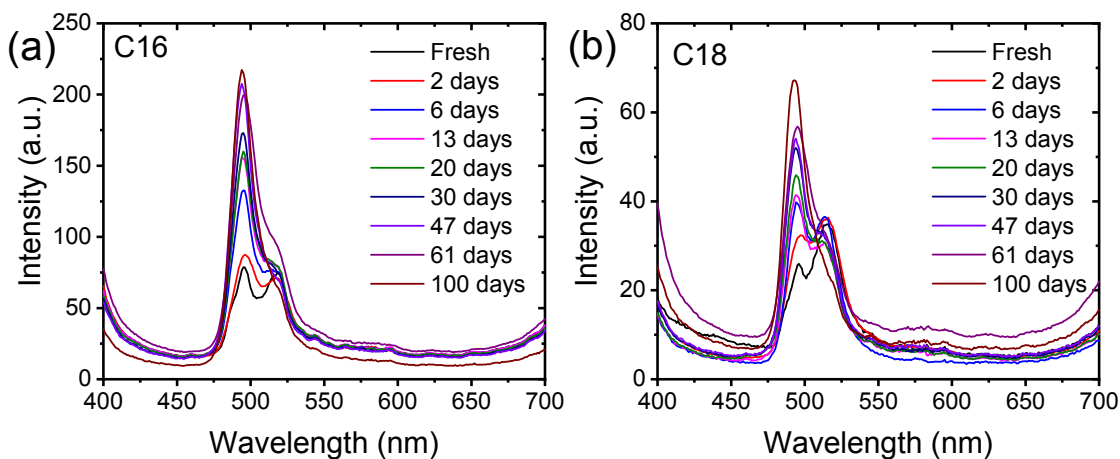


Figure S9. Photoluminescence spectra of thin films of $(C_{16}H_{33}NH_3)_2PbI_4$ and $(C_{18}H_{37}NH_3)_2PbI_4$ 2D perovskite thin films stored under ambient conditions.

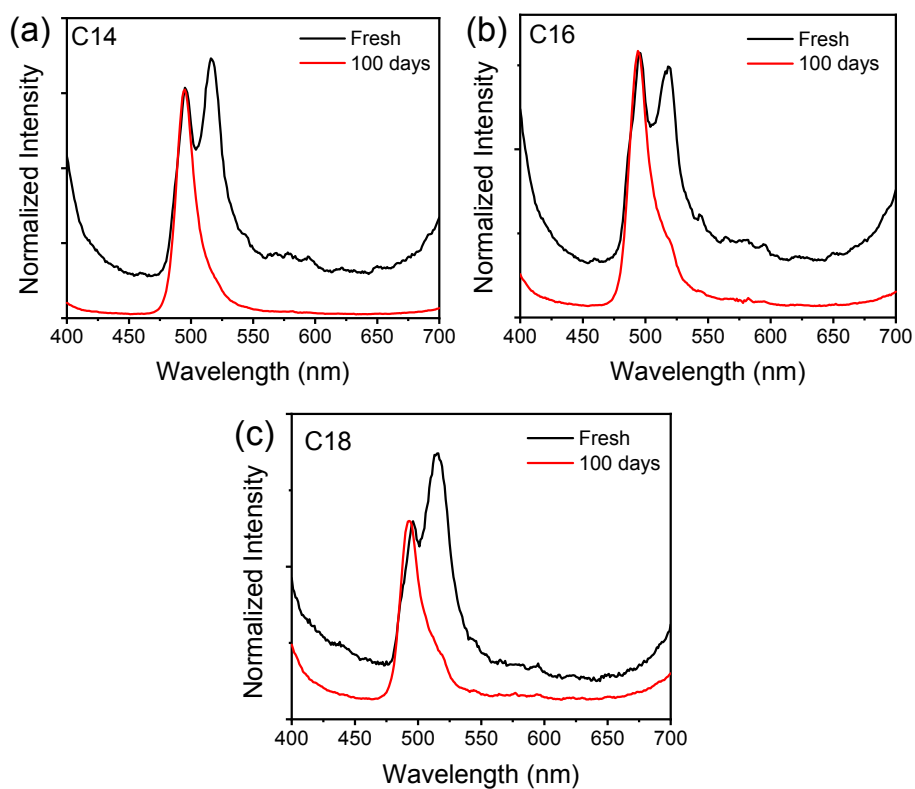


Figure S10. Normalized photoluminescence spectra of fresh and aged thin films of $(C_{14}H_{29}NH_3)_2PbI_4$, $(C_{16}H_{33}NH_3)_2PbI_4$ and $(C_{18}H_{37}NH_3)_2PbI_4$ 2D perovskites stored under ambient conditions.

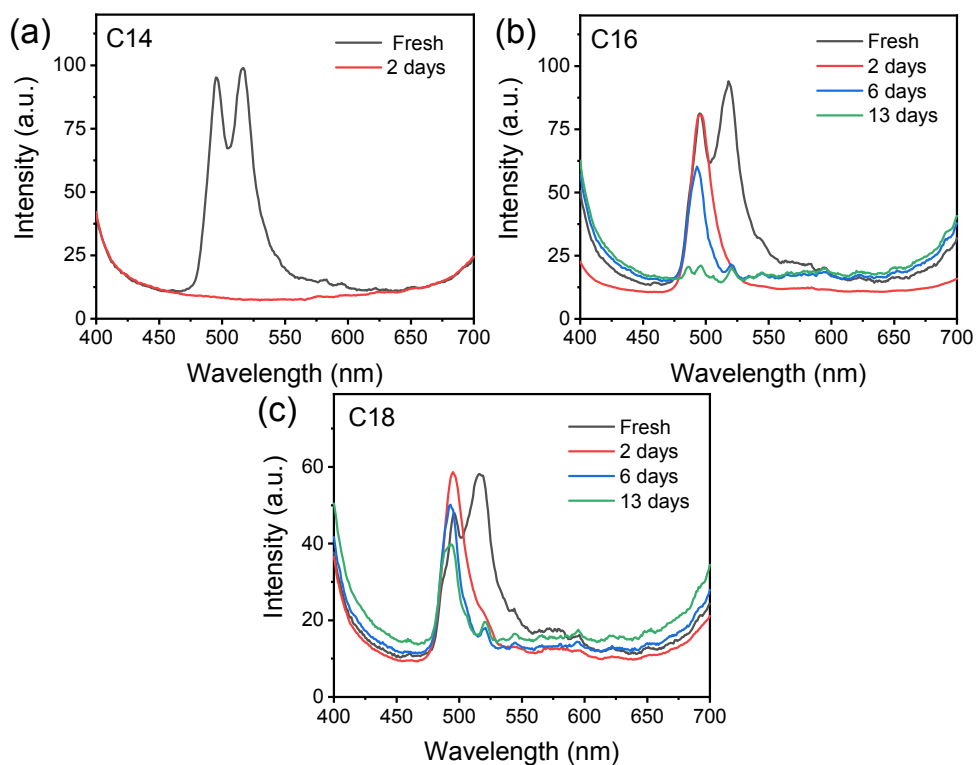


Figure S11. Photoluminescence spectra of thin films of $(\text{C}_{14}\text{H}_{29}\text{NH}_3)_2\text{PbI}_4$, $(\text{C}_{16}\text{H}_{33}\text{NH}_3)_2\text{PbI}_4$ and $(\text{C}_{18}\text{H}_{37}\text{NH}_3)_2\text{PbI}_4$ 2D perovskites immersed in water.

References

1. Billing, D. G.; Lemmerer, A., *New J. Chem.* 2008, **32**, 1736-1746.
2. Barman, S.; Venkataraman, N. V.; Vasudevan, S.; Seshadri, R., *J. Phys. Chem B* 2003, **107**, 1875-1883.
3. Xu-Hui Zhang, Jia-Jiu Ye, Liang-Zheng Zhu, Hai-Ying Zheng, Xue-Peng Liu, Xu Pan, Song-Yuan Dai, *ACS Appl. Mater. Interfaces* 2016, **8**, 35440–35446
4. Christian Würth, Markus Grabolle, Jutta Pauli, Monika Spieles, Ute Resch-Genger, *Nat. Protoc.* 2013, **8**, 1535-1550.